

EXPLORING THE PROPERTIES OF GOLD-SILVER NANOALLOYS CREATED WITH A FEMTOSECOND LASER

#1 **Mr. AMMASI THIRUGNANAM**, *Assistant Professor*

#2 **Mr. SRIPERUMBUDUR VENKATA RAM KUMAR**, *Assistant Professor*

Department of Physics,

SREE CHAITANYA INSTITUTE OF TECHNOLOGICAL SCIENCES, KARIMNAGAR, TS.

ABSTRACT

The optical and electrical characteristics of Au-Ag nanoalloys at various volume ratios were investigated in this study. By directly irradiating the gold and silver ions with a femtosecond laser, they were transformed to nanoparticles. Within a quartz cuvette, the samples were subjected to radiation for 10 minutes. For each individual sample, the optical property associated with the peaks of Localized Surface Plasmon Resonance (LSPR) was examined. In addition, the colloids' electrical conductivity was determined by estimating their zeta potential using the dynamic light scattering (DLS) method. The results show that as the volume percentage of Ag and Au in the Au-Ag nanoalloy changed, the LSPR peak shifted to 409 nm for Ag and 530 nm for Au. The progression of the transformation was practically linear. The conductivity measurement shows that Au₀Ag₁₀₀ Ag nanoparticles have the highest value, whereas Au₁₀₀Ag₀ Au nanoparticles have the lowest value. Au-Ag nanoalloy values vary from Au₀Ag₁₀₀ to Au₁₀₀Ag₀. Our findings show that the optical and electrical properties of Au-Ag nanoalloys can be easily altered by varying the volume fractions of the two components.

Keywords: optical properties, electrical properties, Au-Ag nanoalloys, photochemical reduction, femtosecond laser.

1. INTRODUCTION

Nanotechnology has recently expanded in importance and developed a wide range of uses. Scholars are actively searching for innovative materials that have the potential to improve a wide range of technological areas, including but not limited to catalysts, optical and electrical devices, and all disciplines. In response to the global market's demand for a diverse array of nanoparticles (NPs), chemical, physical, and biological manufacturing processes have advanced. There are two methods for creating metal nanoparticles: top-down and bottom-up. The top-down strategy advocates removing substances using physical, mechanical, or chemical processes in order to make nanoparticles. The bottom-up strategy entails clustering nanoparticles atom by atom and molecule by molecule. In this technique, a substance is assembled. Because it accounts for the reduction of chemical precursors in the solution via mechanical waves (such as

ultrasound), reducing agents, and electromagnetic waves, the bottom-up strategy is thought to be the most effective method for regulating and controlling particle size. The photochemical reduction process, which uses a femtosecond laser to create nanoparticles, is gaining popularity among the general population. Because it just uses a dispersion agent and metal salt, this method is environmentally benign. There are no harmful chemicals used. The aforementioned procedure is used to reduce a metal salt to its elemental components, resulting in nanoparticle production. Noble metal nanoparticles (NPs), such as Ag and Au NPs, are highly researched and valued for their capacity to absorb visible light. The LSPR shift is affected by the size, shape, and dielectric constant of the medium around the device. Further research into this mixture is necessary, since it is possible to manufacture Au-Ag nanoalloys by combining the optical, electrical, and catalytic capabilities of Ag and Au NPs through a modification in their

combination. Furthermore, the use of Au-Ag nanoalloys outperforms the capabilities of Au or Ag NPs alone.

As a result, the goal of this research project is to explore the visual properties of mixed Au-Ag nanoalloys generated by photochemical reduction and femtosecond laser. The volume ratio of Au-Ag nanoalloys varies, which affects their Localized Surface Plasmon Resonance (LSPR), which controls their optical properties. Given that the LSPR of these alloys can be calibrated between Au and Ag NPs, it indicates that the electric characteristics of Au-Ag nanoalloys can be adjusted between Au and Ag NPs. Furthermore, dynamic laser scattering was used in the current study to estimate the zeta potential and assess the electrical conductivity of the Au-Ag nanoalloys.

2. EXPERIMENT

Chemicals and instrumentation

Au-Ag nanoalloys were created by mixing gold and silver metal ions in different volume ratios using a high-pulsed femtosecond laser for photochemical reduction. During irradiation, this approach generates a considerable amount of solvated electron radicals and hydrogen. Potassium gold (III) chloride ($K[AuCl_4]$, 99.995%, Sigma-Aldrich) and silver nitrate ($AgNO_3$, 99%, Rofa Lab) were mixed to make separate solutions of gold and silver ions. PVP (99.9% purity, Sigma Aldrich) was utilized as a covering material to generate silver and gold ions in water.

Table 1 shows the volumetric concentrations of each gold and silver ion in the solution. The samples are denoted by the symbols x and y, which are represented as AuxAgy. Each sample was placed in a 3 mL glass cuvette and subjected to laser light for ten minutes.

Table 1. AuxAgy is a skill component.

Ratio	(Au:Ag)	Ratio	(Au:Ag)
Au ₀ Ag ₁₀₀	0 mL : 3 mL	Au ₆₀ Ag ₄₀	1.8 mL : 1.2 mL
Au ₁₀ Ag ₉₀	0.3 mL : 2.7 mL	Au ₇₀ Ag ₃₀	2.1 mL : 0.9 mL
Au ₂₀ Ag ₈₀	0.6 mL : 2.4 mL	Au ₈₀ Ag ₂₀	2.4 mL : 0.6 mL
Au ₃₀ Ag ₇₀	0.9 mL : 2.1 mL	Au ₉₀ Ag ₁₀	2.7 mL : 0.3 mL
Au ₄₀ Ag ₆₀	1.2 mL : 1.8 mL	Au ₁₀₀ Ag ₀	3 mL : 0 mL
Au ₅₀ Ag ₅₀	1.5 mL : 1.5 mL		

The method used a Ti-sapphire femtosecond laser (Spitfire Ace, Spectra-Physics) to generate 100 fs full-width-half-maximum (FWHM) pulses at 800 nm. The power of each pulse was 2.1 Watts, and the repetition frequency was 1 kHz. Figure 1 depicts the undertaking's organizational structure. Using UV-Vis spectrophotometry (MayaPro 2000, Ocean Optics), we analyzed the Localized Surface Plasmon Resonance (LSPR) peaks of each sample that had been subjected to radiation. A particle size detector (PSA Nano Plus 3, Micromeritics USA) was also used to determine the conductivity and zeta potential of the colloids. The material's crystalline structure and morphology were then investigated using transmission electron microscopy (TEM FEI Tecnai G 20 S-Twin, 200kV) and X-ray diffraction (XRD, Rigaku Smartlab 3kW).

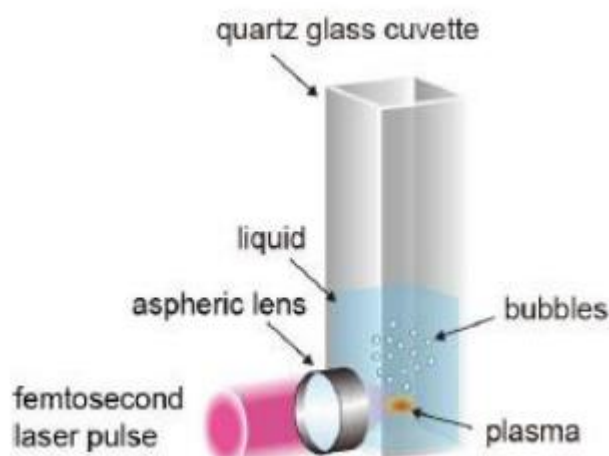


Figure 1. Diagram of the prototype configuration.
Procedure reaction

1 gram of silver nitrate ($AgNO_3$, 99%, Rofa Lab) and 100 mL of potassium gold (III) chloride ($K[AuCl_4]$, 99.995%, Sigma-Aldrich) were mixed with filtered water to make a solution containing gold and silver ions at concentrations of 4.22×10^{-4} M. To promote the creation of nanoparticles, 100 mL of $AgNO_3$ solution was treated with 0.01 l of

ammonia (NH₄OH, 25% by weight, Rofa Lab). More than 0.01 grams of polyvinylpyrrolidone (PVP) from Sigma-Aldrich were added to 100 milliliters of 99.9% pure gold and silver ions.

3. RESULT AND DISCUSSION

The use of a femtosecond laser on a solution containing Ag and Au ions resulted in a variety of volume ratios of Au-Ag nanoalloys. Through the emission of many photons, a powerful femtosecond laser promotes ionization in the solvent molecules, resulting in a chemical interaction with the solvent. This interaction produces highly reactive species that are beneficial for beginning chemical reactions in the solution (see Figure 2). Solvated electrons (e_{aq}⁻), hydroxyl radicals (OH•), hydrogen radicals (H•), and hydronium cations (H₃O⁺) have enough energy to destroy metal ions in solution. The short-lived ions e_{aq}⁻ and H• were the most effective reducing agents among all ions dissolved in water. When exposed to radiation, the strong reducing agent would convert metallic M⁺ cations in the solution to M⁰ atoms. These atoms would then precipitate as nanoparticles. The rationale is illustrated in Figure 3. It is conceivable to create a homogeneous alloy by submitting two metal precursors with differing reduction potentials to extremely strong femtosecond laser light. This is because the reduction agent decreases the amount of metal cations. The creation of a homogenous nanoalloy is more likely in systems including Au and Ag components, which mix easily using a phase diagram.

Figure 4 depicts the UV-Vis absorption spectra, Localized Surface Plasmon Resonance peaks as a function of volume ratio, and colloidal alloy nanoparticles generated after ten minutes of exposure. The LSPR peaks in Au-Ag nanoalloys at 530 nm and 409 nm were discovered to be caused by the Localized Surface Plasmon Resonance of silver nanoparticles (Au₀Ag₁₀₀). These peaks are gold nanoparticles made up of Au₁₀₀Ag₀. Figure 4b depicts the roughly linear transition that the LSPR goes through.

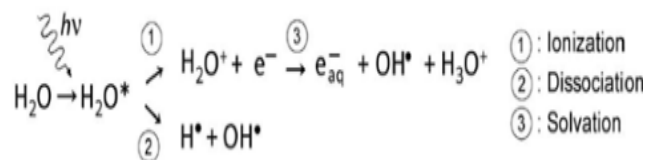


Figure 2 The initial events that occur following the absorption of multiphotons by water molecules using femtosecond laser energy.

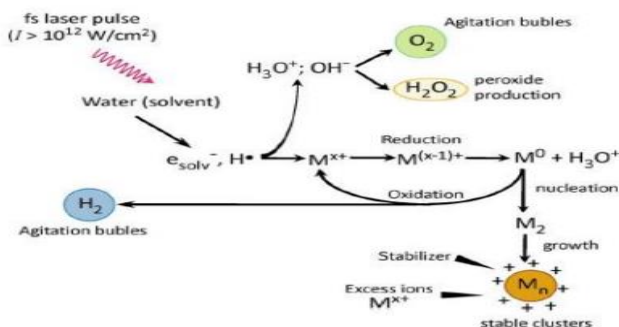


Figure 3. Using a schematic strategy, a highly powerful femtosecond laser promotes the production of nanoparticles in water.

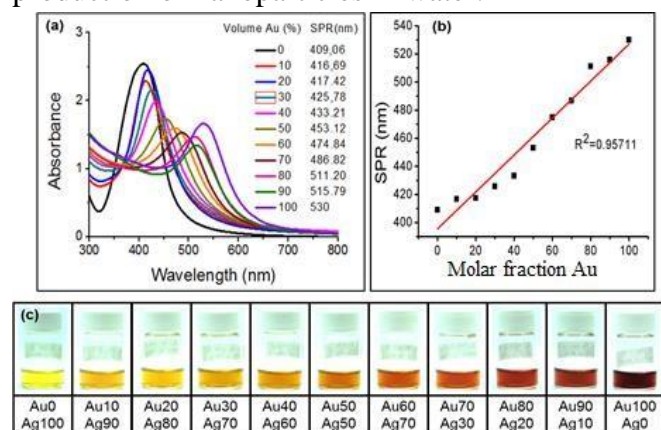


Figure 4. A) UV-Vis absorption spectra; (B) LSPR peaks as a function of Au³⁺ volume fraction; and (C) a femtosecond laser pulse illustration used in the synthesis of colloidal Au-Ag nanoalloys.

The DLS approach was also used to evaluate the electrical properties of the Au-Ag nanoalloys, such as conductivity and zeta potential. The results are shown in Table 2, and they show that pure Ag NPs have higher conductivity than pure Au NPs. The conductivities of the nanoalloys Au₅₀Ag₅₀, Au₂₀Ag₈₀, and Au₈₀Ag₂₀ are comparable to Ag NPs and Au NPs and fall within the intermediate range.

Table 2. Au-Ag nanoalloys' zeta potential and electrical conductivity!.

Sample	Zeta Potential (mV)	Conductivity (mS/cm)
Au0Ag100	-37.1	0.294
Au20Ag80	-23.5	0.291
Au50Ag50	-25.5	0.283
Au80Ag20	-26.5	0.265
Au100Ag0	-12.5	0.253

Furthermore, XRD was used exclusively to collect diffraction data on Au0Ag100 (gold nanoparticles), Au50Ag50, and Au100Ag0 (silver nanoparticles). Using the XRD diffractogram shown in Figure 5, we demonstrated that the purified nanoparticles and their alloy had the same fcc (facial center cubic) crystal structure and lattice planes (111), (200), (220), (311), and (222). In lieu of a core-shell or asymmetrical alloy structure, Au-Ag nanoalloys formed a homogeneous colloid due to the absence of a recently discovered lattice constant.

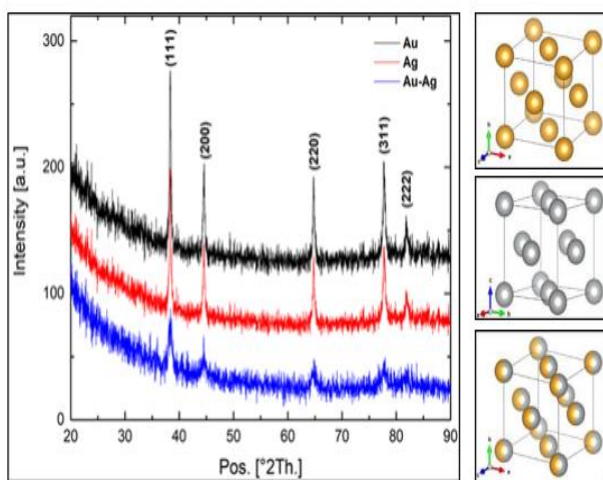


Figure 5. An XRD examination of the appearance, lattice constant, and crystal structure of Au-Ag nanoalloys

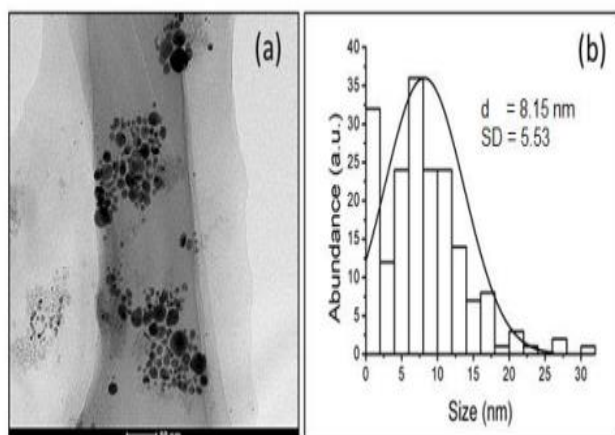


Figure 6. The following photos demonstrate TEM scans of Au50Ag50 nanoalloys subsequent to a ten-minute radiation exposure interval.

The ten-minute exposure of the Au50Ag50 nanoalloys to light subsequent to their synthesis via femtosecond laser is demonstrated in Figure 6. The particle size distribution of the Au50Ag50 nanoalloys is irregular, ranging from less than 5 nm to approximately 30 nm. The average size of nanoparticles is 8.15 ± 5.53 nm. Additionally, the transmission electron microscope image demonstrates the production of metals with a uniform shape. This is further supported by the fact that the UV-Vis spectra of the alloys exhibit a solitary LSPR peak, as opposed to the dual peaks observed in the spectra of core-shell nanoparticles. Indeed, the aforementioned system's femtosecond laser reduction process completed the transformation of metal ions into metal atoms in a mere five minutes. Lasers exhibit their dissolving effect when the duration of laser exposure is prolonged to ten minutes. The laser's heat will cause the nanoparticles to dissolve, thereby reducing their size. Throughout the procedure, numerous nanoparticles may assemble, resulting in an inconsistent distribution of particle sizes.

As illustrated in Figure 4, the LSPR of Au-Ag nanoalloys may differ from that of Au NPs and Ag NPs. Additionally, Table 1 illustrates that the conductivity of Au-Ag nanoalloys is modifiable within the conductivity range of Au and Ag. The findings indicate that it is possible to modify the electrical and visual characteristics of Au-Ag nanoalloys in order to achieve a balance between the attributes of Ag and Au NP.

By combining solutions containing varying quantities of silver and gold ions, we synthesized Au-Ag nanoalloys utilizing the factors AuxAgy, which represent the volume percentage of silver ions in x and gold ions in y. Gaudry et al. discovered that the volume ratio affects the dielectric constant of AuxAgy, which decreases from 38.5 -cm for Au to 19.4 $\mu\Omega$ -cm for Ag. Volume-dependent variations in the dielectric constant had an impact on the LSPR of Au-Ag nanoalloys. Due to the relationship between dielectric constant and electrical conductivity, LSPR tuning (as shown in Table 2) may be

capable of altering the electrical conductivity of Au-Ag nanoalloys. This may promote the development of these materials for a greater variety of applications.

4. CONCLUSION

Using a femtosecond laser and ten minutes of photochemical reduction, Au-Ag nanoalloys could be produced from a solution containing gold and silver metal particles. Utilizing XRD, DLS, and UV-Vis spectroscopy, the colloids were analyzed. Evidently, it is possible to modify the optical and electrical properties of Au-Ag nanoalloys in order to achieve an equilibrium between the attributes of Ag and Au NP. By modifying the optical characteristics of Au-Ag nanoalloys, one can obtain conductivity and LSPR values ranging from 0.253 to 0.294 mS/cm and 409.06 to 530 nm, respectively. This study's results indicate that Au-Ag nanoalloys might have a broader range of applications than pure Au and Ag nanoparticles.

REFERENCES

1. Choi, H., Ko, S. J., Choi, Y., Joo, P., Kim, T., Lee, B. R., Jung, J. W., Choi, H. J., Cha, M., Jeong, J. R., and Hwang, I. W., *Nat. Photonics*, 2013, 7(9), 732-738.
2. Upender, G., Satyavathi, R., Raju, B., Alee, K. S., Rao, D., and Bansal, C., *Chem. Phys. Lett.*, 2011, 511(4-6), 309-314.
3. Lee, J., Mahendra, S., Alvarez, P.J., *ACS Nano*, 2010, 4(7), 3580-3590.
4. Yang, Z., Ren, J., Zhang, Z., Chen, X., Guan, G., Qiu, L., Zhang, Y., and Peng, H., *Chem. Rev.*, 2015, 115(11), 5159-5223.
5. Zhang, X. F., Liu, Z. G., Shen, W., and Gurunathan, S., *Int. J. Mol. Sci.*, 2016, 17(9), 1534.
6. Itina, T. E., *J. Phys. Chem. C.*, 2011, 115(12), 5044-5048.
7. Johnston, R. L., *Metal Nanoparticles and Nanoalloys*, in *Frontier of Nanoscience*, 2012, 3, Elsevier, Birmingham.
8. Thakkar, K. N., Mhatre, S. S., and Parikh, R. Y., *Nanomedicine*, 2010, 6(2), 257 - 262.
9. Herbani, Y., Nakamura, T., and Sato, S., *J. Phys. Chem. C*, 2011, 115(44), 21592-21598.
10. Gopinath, V., Priyadarshini, S., Loke, M. F., Arunkumar, J., Marsili, E., Ali, D., M.,

Velusamy, P., and Vadivelu, J., *Arab. J. Chem.*, 2017, 10 (8), 1107-1117.

10. Sonnichsen, C., Reinhard, B. M., Liphardt, J., and Alivisatos, A. P., *Nat. Biotechnol.*, 2005, 23(6), 741-745.

11. Link, S., and El-Sayed, M.A., *J. Phys. Chem. B*, 1999, 103(21), 4212-4217.

Wang, A.Q., Chang, C.M. and Mou, C.Y., *J. Phys. Chem B*, 2005, 109(40), 18860-18867.